




Bacterial Cytological Profiling Identifies Rhodanine-Containing PAINS Analogs as Specific Inhibitors of *Escherichia coli* Thymidylate Kinase *In Vivo*

Elizabeth T. Montaña,^a Jason F. Nideffer,^a Joseph Sugie,^a Eray Enustun,^a  Adam B. Shapiro,^b Hannah Tsunemoto,^a Alan I. Derman,^a Kit Pogliano,^a Joe Pogliano^a

^aDivision of Biological Sciences, University of California—San Diego, La Jolla, California, USA

^bEntasis Therapeutics, Gatehouse Park BioHub, Waltham, Massachusetts, USA

Elizabeth T. Montaña and Jason F. Nideffer contributed equally to this article. Their names were ordered alphabetically by last name.

ABSTRACT In this study, we sought to determine whether an *in vivo* assay for studying antibiotic mechanisms of action could provide insight into the activity of compounds that may inhibit multiple targets. Thus, we conducted an activity screen of 31 structural analogs of rhodanine-containing pan-assay interference compounds (PAINS). We identified nine active molecules against *Escherichia coli* and classified them according to their *in vivo* mechanisms of action. The mechanisms of action of PAINS are generally difficult to identify due to their promiscuity. However, we leveraged bacterial cytological profiling, a fluorescence microscopy technique, to study these complex mechanisms. Ultimately, we found that although some of our molecules promiscuously inhibit multiple cellular pathways, a few molecules specifically inhibit DNA replication despite structural similarity to related PAINS. A genetic analysis of resistant mutants revealed thymidylate kinase (essential for DNA synthesis) as an intracellular target of some of these rhodanine-containing antibiotics. This finding was supported by *in vitro* activity assays, as well as experiments utilizing a thymidylate kinase overexpression system. The analog that demonstrated the half-maximal inhibitory concentration *in vitro* and MIC *in vivo* displayed the greatest specificity for inhibition of the DNA replication pathway, despite containing a rhodamine moiety. Although it is thought that PAINS cannot be developed as antibiotics, this work showcases novel inhibitors of *E. coli* thymidylate kinase. Moreover, perhaps more importantly, this work highlights the utility of bacterial cytological profiling for studying the *in vivo* specificity of antibiotics and demonstrates that bacterial cytological profiling can identify multiple pathways that are inhibited by an individual molecule.

IMPORTANCE We demonstrate that bacterial cytological profiling is a powerful tool for directing antibiotic discovery efforts because it can be used to determine the specificity of an antibiotic's *in vivo* mechanism of action. By assaying analogs of PAINS, molecules that are notoriously intractable and nonspecific, we (surprisingly) identify molecules with specific activity against *E. coli* thymidylate kinase. This suggests that structural modifications to PAINS can confer stronger inhibition by targeting a specific cellular pathway. While *in vitro* inhibition assays are susceptible to false-positive results (especially from PAINS), bacterial cytological profiling provides the resolution to identify molecules with specific *in vivo* activity.

KEYWORDS *E. coli*, PAINS, SAR, antibiotic, bacterial cytological profiling, mechanism

Due to the increasing emergence of multidrug-resistant (MDR) bacteria, there is a desperate need for new antibiotics to effectively treat persistent infections (1–3). In 2015, ceftazidime-avibactam-resistant *Klebsiella pneumoniae* was identified within months of the antibiotic's approval for use in the clinic (4). In addition, as the rate at

Citation Montaña ET, Nideffer JF, Sugie J, Enustun E, Shapiro AB, Tsunemoto H, Derman AI, Pogliano K, Pogliano J. 2021. Bacterial cytological profiling identifies rhodanine-containing PAINS analogs as specific inhibitors of *Escherichia coli* thymidylate kinase *in vivo*. *J Bacteriol* 203:e00105-21. <https://doi.org/10.1128/JB.00105-21>.

Editor William W. Metcalf, University of Illinois at Urbana Champaign

Copyright © 2021 American Society for Microbiology. All Rights Reserved.

Address correspondence to Joe Pogliano, jpogliano@ucsd.edu.

Received 20 February 2021

Accepted 22 June 2021

Accepted manuscript posted online 19 July 2021

Published 8 September 2021

which pathogens are developing resistance to clinically administered antibiotics continues to increase, many companies once actively involved in antibiotic discovery are abandoning these efforts (5–11). Consequently, the speed at which antibiotics are achieving clinical status is not fast enough to keep pace with evolving resistance (9–11). For this reason, the continued research and development of potential drug candidates is critical for combatting one of the greatest threats to global health today.

Vast libraries of natural products and/or synthetic molecules are frequently screened in order to identify those with antibacterial activity (12). These screens often yield a number of active molecules; however, potent inhibitors are rarely pursued if their mechanisms of action (MOA) are difficult to classify. Consequently, many of these molecules do not make it to the development stage of antibiotic research (13). Pan-assay interference compounds (PAINS) constitute a structurally diverse class of molecules that contain highly reactive functional groups (such as toxoflavin, isothiazolone, curcumin, hydroxyphenol hydrazine, phenol-sulfonamide, or rhodanine) that frequently interfere with the integrity of biological assays and yield false-positive results (14). Their tendency to react with or bind promiscuously to many different targets makes PAINS notoriously difficult to study and, for this reason, they are often discarded from antibiotic investigations (15, 16). In fact, filters have been developed for removing PAINS from compound libraries prior to screening (17). Consequently, many PAINS remain unstudied.

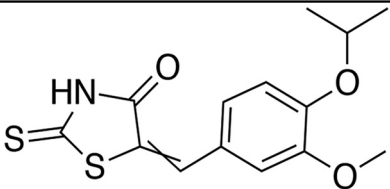
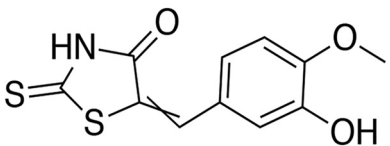
Previously, we developed bacterial cytological profiling (BCP) as a method for rapidly pinpointing the cellular pathway(s) targeted by an antibiotic (18, 19). BCP, which has been used to ascertain the MOA of a variety of compounds active against Gram-negative and Gram-positive bacteria, is predicated on the different cytological changes that occur in cells exposed to antibiotics with various mechanisms (18–22). For example, inhibitors that strongly block protein synthesis (i.e., tetracycline) cause the DNA to assume a toroidal structure, while inhibitors of transcription (i.e., rifampin) cause the DNA to decondense (see Fig. S1 in the supplemental material). Inhibitors of cell wall biogenesis induce cell shape defects and cause lysis, while antibiotics affecting DNA replication (i.e., ciprofloxacin) yield elongated cells that contain a single, centrally located nucleoid. We previously demonstrated that the inhibition of multiple pathways within a single cell results in a combination of distinguishable phenotypes (22, 23). Thus, BCP enables us to study mechanistically complex molecules, which would otherwise present an insurmountable challenge due to their multiple cellular targets or general reactivity. When used for analyses of structure-activity relationships (SAR), BCP facilitates the identification of molecular analogs that have a greater specificity for a single target pathway.

Here, we conducted an antibiotic screen and identified a chemical series of PAINS-related molecules with antibacterial activity against an *Escherichia coli* $\Delta tolC$ strain. With the understanding that PAINS have little direct clinical relevance, we pursued these molecules in order to validate BCP as an approach for studying mechanistically complex antibiotics. Using BCP, we discovered that some PAINS-related molecules inhibit multiple pathways *in vivo*, but other structural analogs exhibited high specificity for the DNA synthesis pathway. *In vivo* and *in vitro* experiments revealed that some of these molecules specifically inhibit thymidylate kinase (TMPK), an essential enzyme that catalyzes the synthesis of dTDP from dTMP (24). Conserved in many bacterial species, TMPK is a promising target for new antibiotics (25). Thus, our study identifies potentially powerful cell biology tools: molecules with specific activity against TMPK in an isolated *E. coli* system, as well as a novel application of BCP for studying families of antibiotics that have long been considered too much of a “pain” to study.

RESULTS AND DISCUSSION

Characterizing the cellular pathways inhibited by two PAINS using BCP and viability studies. A library of 1,798 synthetic small molecules was screened to identify those that inhibit the growth of the *E. coli* $\Delta tolC$ strain. In conducting this screen, we identified two active compounds that shared a similar backbone structure containing a

TABLE 1 Structures and MICs of PAINS compounds 1 and 2

Compound	Structure	<i>E. coli</i> JP313 $\Delta tolC$ MIC (μM)
1		11.7
2		6.1

rhodanine moiety, suggesting that they might be PAINS. These molecules, designated compound 1 and compound 2, are shown in Table 1. The MICs of compounds 1 and 2 against the *E. coli* $\Delta tolC$ strain were determined to be 11.7 and 6.1 μM , respectively. To rapidly identify the pathway(s) inhibited by these compounds, we performed BCP. *E. coli* $\Delta tolC$ cells were treated with each compound at concentrations equivalent to 1 \times , 3 \times , and 5 \times MIC for durations of 30 min, 1, 2, and 4 h. After treatment, the cells were stained with fluorescent dyes and imaged using high-resolution fluorescence microscopy (Fig. 1). Cells treated with compound 1 at 3 \times and 5 \times MIC for 2 h or more were elongated and contained a single, centrally located nucleoid (Fig. 1A), resembling cells treated with known DNA replication inhibitors (see Fig. S1) (19–22). At these concentrations, some cells also appeared to be swollen or lysed, typical of cells treated with cell wall inhibitors. Compound 2 also induced DNA replication defects after 1 h of treatment at all tested concentrations, and a severe degree of cell lysis and spheroplast formation were observed after 4 h of treatment (Fig. 1B, arrows). Thus, consistent with the knowledge that PAINS often target multiple pathways, compounds 1 and 2 inhibited two distinct metabolic processes, DNA replication and cell wall biogenesis.

Our viability experiments further characterized the antibacterial effects of compounds 1 and 2 against *E. coli* $\Delta tolC$. Compound 1 appeared to be largely bacteriostatic, for even when cells were treated at 5 \times MIC, viability never decreased considerably (Fig. 2A). Compound 2, on the other hand, caused more than a 10-fold average reduction in the number of viable *E. coli* $\Delta tolC$ cells after treatment at 5 \times MIC (Fig. 2B). These data are consistent with our BCP observations because, while both compounds inhibited DNA replication, compound 2 caused more significant cell lysis and appeared to inhibit cell wall biogenesis to a much greater degree (Fig. 1B, arrows).

Identifying TMPK as a cellular target by isolating resistant mutations and performing *in silico* docking. Though we suspected that compounds 1 and 2 inhibited the DNA replication pathway, we did not know which protein within the pathway was inhibited. To identify a potential enzymatic target, we passaged *E. coli* $\Delta tolC$ serially in the presence of increasing concentrations of both compounds and obtained one resistant mutant for each compound. The MIC of compound 1 against its corresponding resistant mutant (mutant 1) was six times higher than the MIC against the *E. coli* $\Delta tolC$ parent strain, and mutant 1 was also resistant (~ 2.8 -fold) to compound 2 (Table 2). Mutant 2 (from compound 2) was roughly 10-fold resistant to both compounds. Whole-genome sequencing revealed that both resistant mutants contained missense mutations in the *tmk* gene, which codes for TMPK (see Fig. S2). In mutant 1, proline replaced glutamine at residue 45, and in mutant 2, threonine replaced alanine at residue 69. Mutant 1 contained an additional mutation in the *dksA* gene, and mutant 2 contained an additional mutation in the *yjeA* gene. However, because *tmk* was the

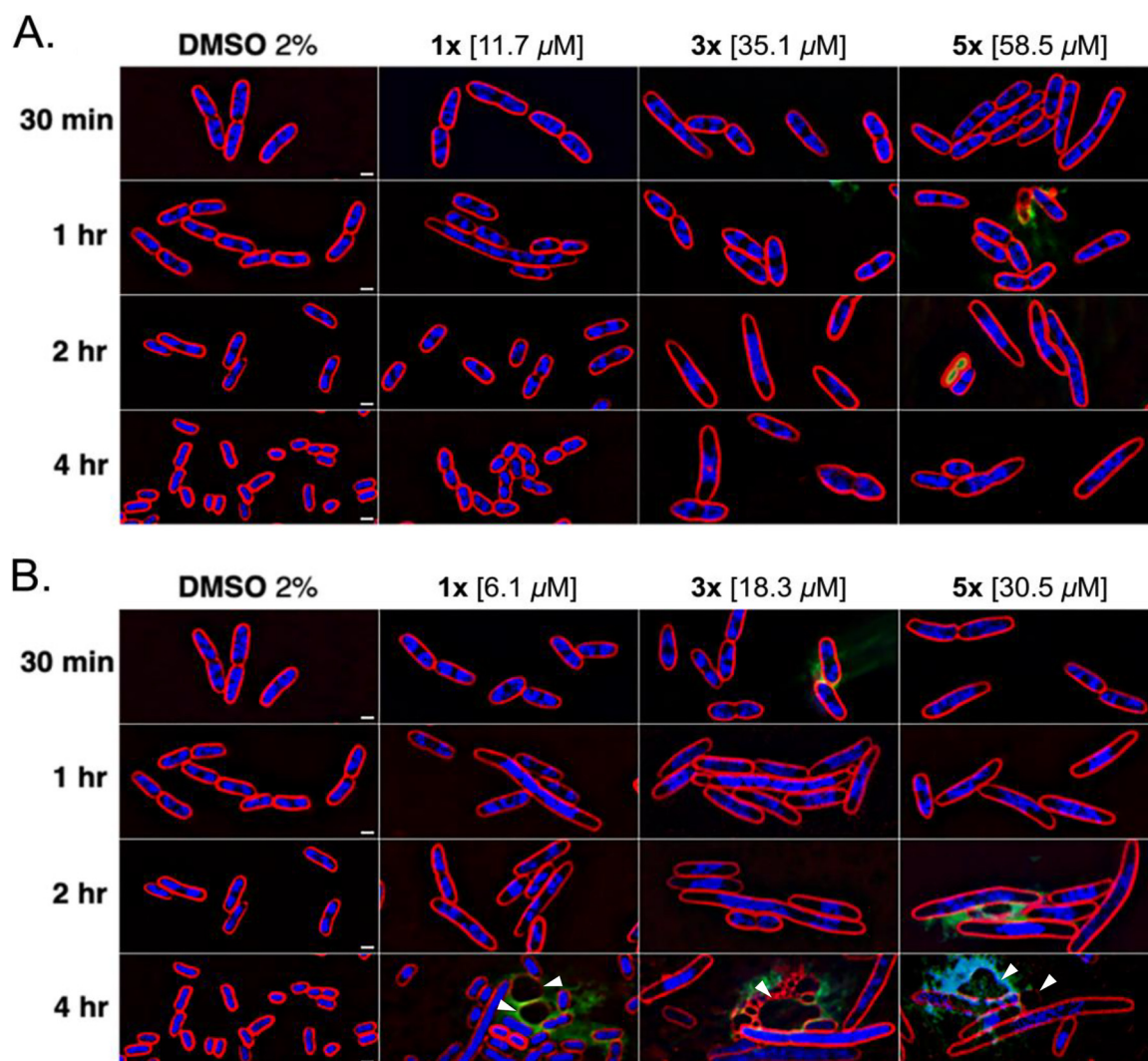


FIG 1 Cytological profiles of the *E. coli* JP313 $\Delta tolC$ strain treated with two PAINS. Cells were exposed to compound 1 (A) or compound 2 (B) at 1 \times , 3 \times , and 5 \times MIC for 30 min, 1 h, 2 h, and 4 h. Images were taken after staining the cells with FM4-64 (red), DAPI (blue), and SYTOX-green (green). Arrowheads mark spheroplasts indicative of inhibited cell wall biogenesis. Scale bars, 1 μ m.

only gene that was mutated in both strains and because cross-resistance was conferred, we suspected that these mutated *tmk* alleles were likely responsible for conferring some resistance to the compounds. Therefore, we moved the *tmk* allele from the more resistant mutant into a clean strain background via phage P1 transduction. In isolation, the *tmk(A69T)* allele conferred 6-fold resistance to compound 1 and 2.4-fold resistance to compound 2 (Table 2). These results suggest that TMPK is a cellular target of both compounds *in vivo*.

In order to probe the potential molecular mechanism of our compounds, we used computational modeling to dock compounds 1 and 2 to TMPK (Fig. 3). This analysis revealed binding sites for compounds 1 and 2 that overlap considerably within the TMPK active site. The high-probability binding orientation of our inhibitors closely mimicked that of the substrate (dTMP) and known analog inhibitors (26, 27). It is likely that by binding at this location, compounds 1 and 2 compete with dTMP binding and block the enzyme's catalytic activity. Neither of the resistant mutations that we selected was located in the TMPK active site, and it remains unclear how these mutations confer resistance to compounds 1 and 2.

Screening analogs of compounds 1 and 2. In order to identify specific inhibitors of TMPK, we screened 29 structural analogs of compounds 1 and 2 for their antibacterial

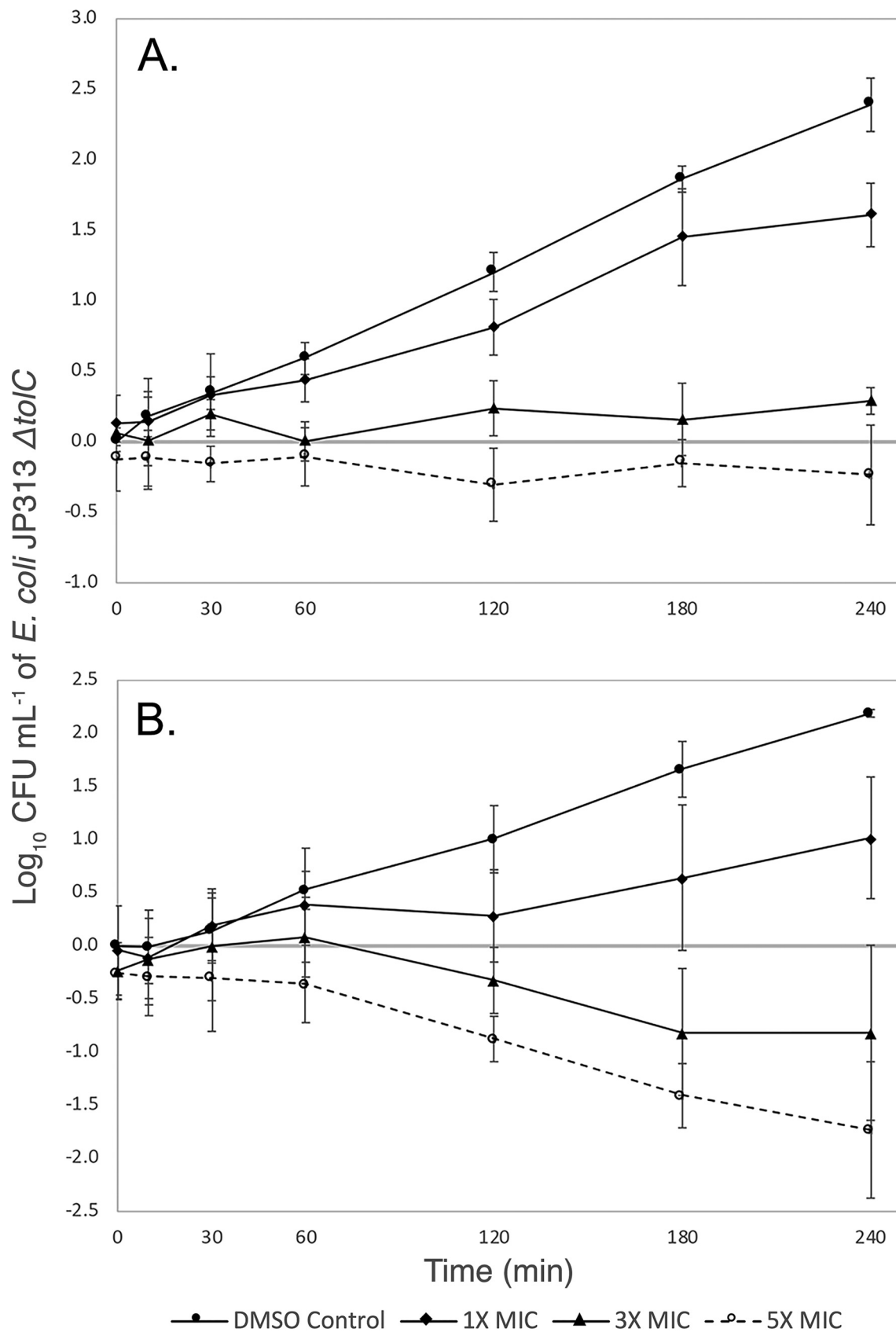


FIG 2 Viability of the *E. coli* JP313 $\Delta tolC$ strain treated with two PAINS. Cells were treated with various concentrations of compound 1 (A) or compound 2 (B). CFU/ml was measured at 30 min, 1 h, 2 h, 3 h, and 4 h. Standard errors were calculated from three independent trials.

TABLE 2 MICs of compounds 1 and 2 against resistant mutants

Strain	MIC (μM)	
	Compound 1	Compound 2
<i>E. coli</i> JP313 ΔtolC	11.7	6.1
<i>E. coli</i> JP313 ΔtolC mutant 1	75.0	17.2
<i>E. coli</i> JP313 ΔtolC mutant 2	>100	81.0
<i>E. coli</i> JP313 ΔtolC <i>tmk(A69T)</i>	68.8	14.8

activity and MOA against the *E. coli* ΔtolC mutant (see Fig. S3). Of these analogs, seven showed antibacterial activity with MICs less than $50\ \mu\text{M}$ (Table 3; see also Table S1 in the supplemental material). Compound 27 was the most potent, with an MIC of $1.9\ \mu\text{M}$. BCP was used to determine whether these analogs inhibit DNA replication specifically or have other mechanisms of action (Fig. 4). Many of the compounds induced filamentation and chromosomal replication defects, indicating that they inhibit DNA replication (Fig. 4), but most of these molecules also inhibited other pathways, such as cell wall biogenesis, which was evidenced by cell lysis. Compound 13 induced membrane permeability and cell lysis with no sign of inhibited DNA replication. This compound had a relatively high MIC compared to most other active molecules. In addition to nonspecific inhibitors, we identified three molecules (compounds 9, 11, and 27) that selectively inhibited DNA replication. The molecule with perhaps the most promise as a TMPK inhibitor was compound 27, since it displayed the lowest MIC and a clear cytological profile indicating high specificity for the DNA replication pathway.

Testing mutant and plasmid-overexpressing strains for resistance to analogs.

To provide evidence that TMPK is the molecular target of some of our PAINS analogs, we tested the activity of these molecules against the *tmk(A69T)* mutant strain. This mutant exhibited some degree of resistance to all of the analogs (Table 4). The MIC of compound 27 was most drastically increased (10-fold) in the *E. coli* strain containing *tmk(A69T)*, further suggesting that this analog specifically inhibits thymidylate kinase *in vivo*. Conversely, those analogs that appeared not to inhibit DNA replication as strongly since

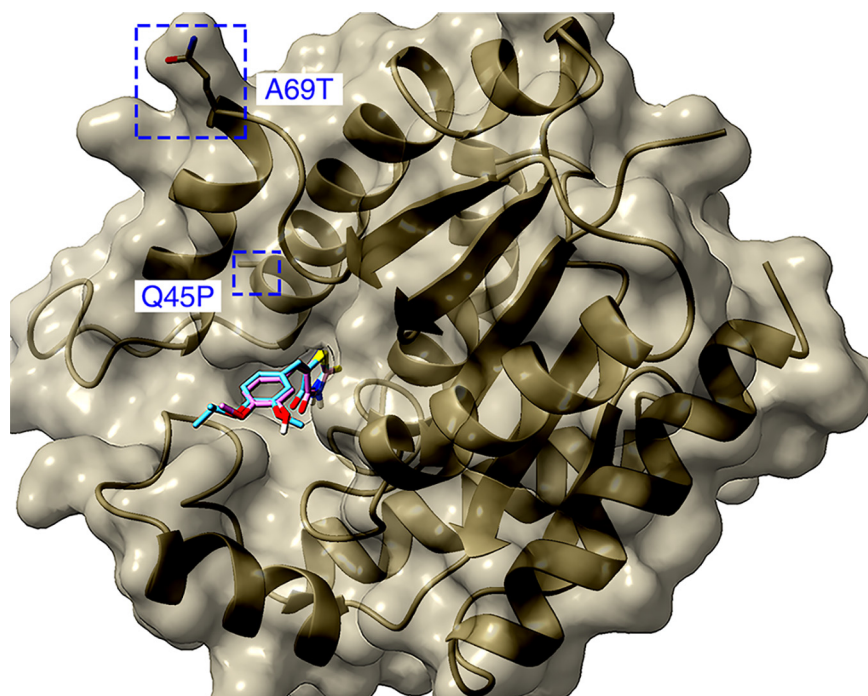
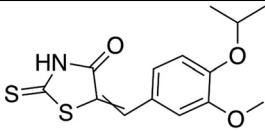
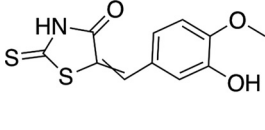
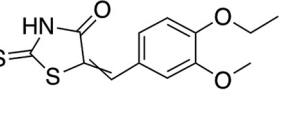
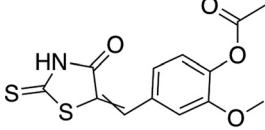
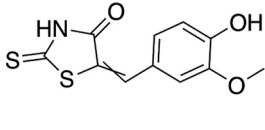
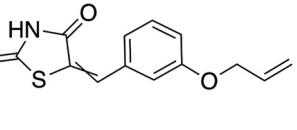
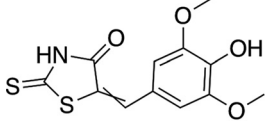
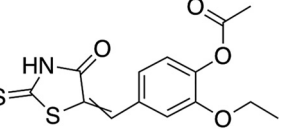
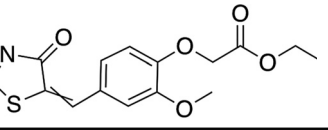


FIG 3 Compounds 1 and 2 docked to the active site of TMPK. Compound 1 (cyan) and compound 2 (magenta) are shown overlapping. Mutated residues conferring resistance are labeled in blue. Heteroatoms are colored such that sulfur is yellow, oxygen is red, and nitrogen is blue.

TABLE 3 Structures and MICs of PAINS analogs

Compound	Structure	<i>E. coli</i> JP313 Δ tolC MIC (μ M)
1		11.7
2		6.1
9		11.7
11		14.1
12		9.0
13		28.1
27		1.9
28		7.8
31		43.7

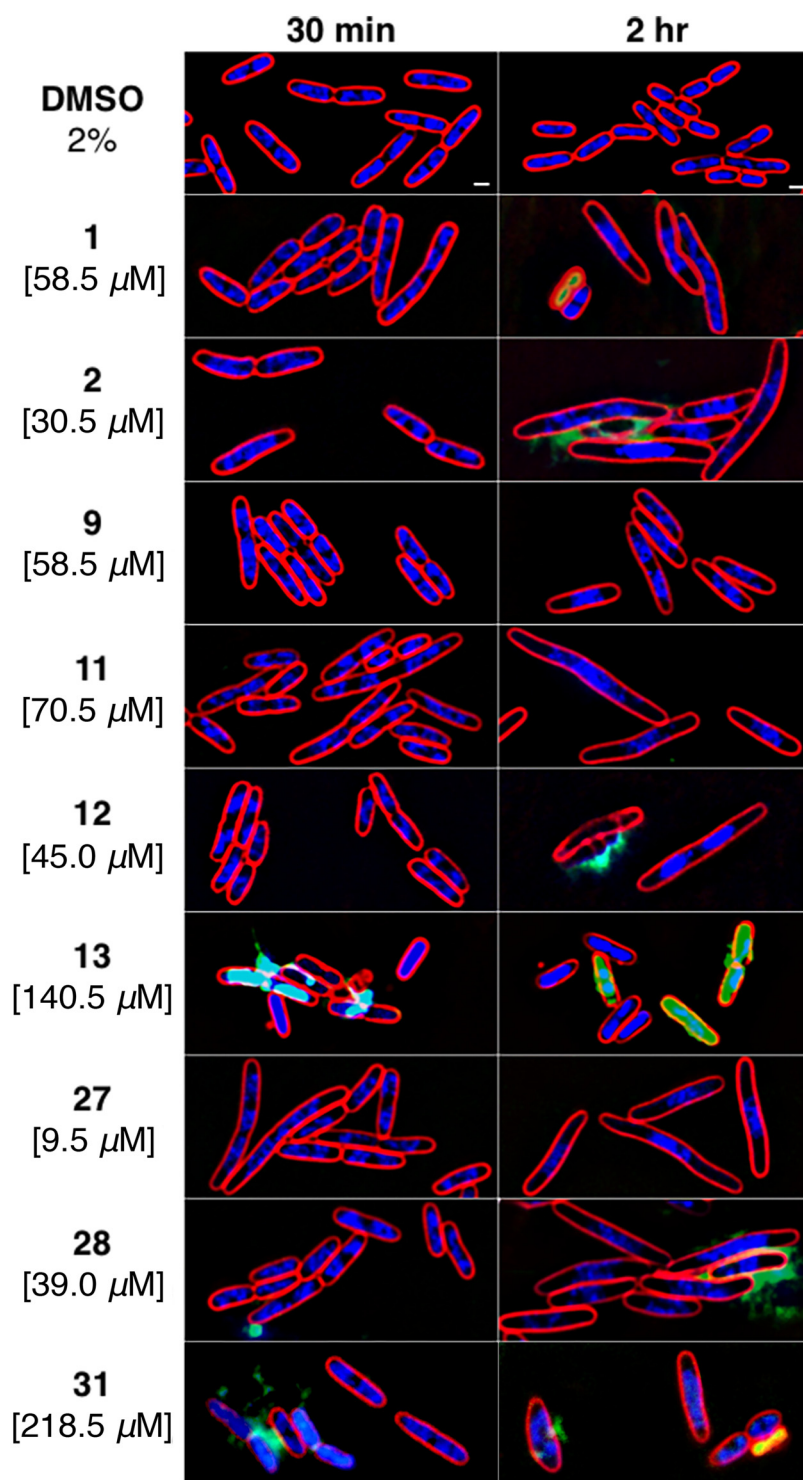


FIG 4 Cytological profiles of the *E. coli* JP313 $\Delta tolC$ strain treated with PAINS analogs. *E. coli* JP313 $\Delta tolC$ cells were treated with 2% DMSO as a control. Analogs were administered at 5 \times MIC (concentrations shown on the left), and images were taken after 30 min and 2 h. Scale bars, 1 μ m.

compound 27 showed only a modest increase in MIC against the *tmk(A69T)* strain. For example, the MICs of compounds 13 and 31 were only \sim 2-fold higher against this strain compared to the strain with wild-type *tmk*.

To provide additional evidence that thymidylate kinase might be the target of this family of compounds, we tested whether TMPK overexpression conferred resistance.

TABLE 4 MICs of PAINS analogs against *E. coli* $\Delta tolC$ *tmk(A69T)* and plasmid-overexpressing strains, as well as IC₅₀ values for the inhibition of *E. coli* TMPK *in vitro*

Compound ^a	Allele-conferred resistance (μ M)			Plasmid overexpression (μ M)				<i>In vitro</i> inhibition (μ M) <i>E. coli</i> TMPK IC ₅₀
	<i>E. coli</i> $\Delta tolC$ <i>tmk</i> ⁺	<i>E. coli</i> $\Delta tolC$ <i>tmk(A69T)</i>	Conferred fold resistance	Vector control	Plasmid+ <i>tmk</i>	Plasmid+ <i>tmk(Q45P)</i>	Plasmid+ <i>tmk(A69T)</i>	
1	11.7	68.8	5.9	15.5	62	62	62	0.39
2	6.1	14.8	2.4	7.8	31	62	62	2.50
8 ^a	>100							1.20
9	11.7	43.8	3.7	15.5	62	62	62	0.41
11	14.1	37.5	2.7	15.5	62	>62	>62	0.48
12	9.0	20.3	2.3	7.8	31	>62	>62	0.50
13	28.1	56.3	2.0	31.3	62.5	62.5	62.5	1.00
14*	>100							4.20
16*	>100							5.60
27	1.9	18.8	10	3.9	15.5	15.5	15.5	0.25
28	7.8	19.4	2.5	7.8	31.3	64	64	0.47
31	43.7	93.8	2.1	31.3	125	125	125	0.68

^a*, inactive *in vivo*.

To accomplish this, we cloned the wild-type *tmk* gene, as well as the *tmk(A69T)* and *tmk(Q45P)* resistant alleles, on multicopy number plasmids and measured the MICs of all nine of our active compounds against the *E. coli* $\Delta tolC$ mutant transformed with these plasmids. Overexpression of the wild-type or mutant *tmk* genes resulted in at least a 4-fold increase in the MICs of all compounds with BCP phenotypes characteristic of DNA replication inhibitors (Table 4). In the cases of compounds 2, 12, and 28, an even greater increase in MIC (up to 8-fold) was observed when either *tmk(A69T)* or *tmk(Q45P)* was overexpressed. In contrast, the MIC of compound 13, which had no obvious effect on DNA replication *in vivo*, was increased only 2-fold upon overexpression of *tmk* alleles.

PAINS analogs inhibit thymidylate kinase *in vitro*. Because our genetic and cell biology studies suggested that thymidylate kinase is a target of this family of molecules, we determined whether or not these compounds inhibited the purified *E. coli* thymidylate kinase *in vitro*. We obtained 50% half-maximal concentrations (IC₅₀; indicating 50% inhibition of purified TMPK activity *in vitro*) for all nine active compounds and also for three compounds with no activity against the *E. coli* $\Delta tolC$ mutant (compounds 8, 14, and 16) (Table 4). The inactive compounds studied were chosen on the basis of their structural diversity. The IC₅₀ values for all 12 compounds ranged from 250 nM (compound 27) to 5.6 μ M (compound 16) (Table 4). As might be expected, the three compounds for which MICs could not be measured had some of the highest IC₅₀ values and yielded poor dose-response curves (see Fig. S4). Compound 27, which is the most potent and specific inhibitor *in vivo*, displayed the lowest IC₅₀. Despite this, our data seemed to demonstrate only a weak positive correlation between compound MIC and IC₅₀. This correlation was primarily affected by the unexpectedly high IC₅₀ value associated with compound 2, one of the strongest inhibitors *in vivo*. The *r*² value for the linear correlation between IC₅₀ values and MICs was 0.001; however, the removal of compound 2 yielded a significantly improved value of 0.536 (see Fig. S5A and B). In addition, an analysis of the relationship between IC₅₀ values and MICs using logistic regression yielded a pseudo *r*² value of 0.246 with the inclusion of compound 2 but achieved perfect separation (pseudo *r*² value of 1.0) when compound 2 was excluded (see Fig. S5C and D). We suspect that compound 2 disrupts the correlation between IC₅₀ values and MICs because it inhibits non-TMPK targets with greater potency than the other molecules. Of the compounds that appeared based on BCP to inhibit cell wall biogenesis, compound 2 was the most potent. In addition, the *tmk(A69T)* mutation conferred only 2.4-fold resistance against compound 2, whereas mutant 2 which contained this mutation and one additional mutation in *yjeA* was >13-fold resistant. Together, these data suggest that TMPK is likely not the primary target of compound 2 and therefore that compound 2 should not be expected to contribute to the

correlation between MICs and IC₅₀ values against purified TMPK. That being said, inconsistencies between MICs and IC₅₀ values could potentially be explained by other factors. For instance, the cell envelope is a significant barrier to antibiotic infiltration, and different structural features of our antibiotic analogs could affect their ability to enter the cell (28). In addition, some of these molecules might behave as PAINS and yield misleading data when studied using *in vitro* assays such as this one.

Here, we present a collection of genetic, cell biological, and biochemical data that demonstrate that many of the molecules within a particular rhodanine-containing chemical series inhibit cellular TMPK. Although some of these molecules have additional targets *in vivo*, three compounds appeared to specifically target TMPK. Compound 27, stands out among this group because, in addition to its specificity (eliciting clear DNA replication defects *in vivo*), it had the most potent IC₅₀ against the purified protein *in vitro* and inhibited the growth of the *E. coli* $\Delta toIC$ mutant with the lowest MIC. It may be the case that PAINS cannot be developed as antibiotics, for even if compounds with specific antibacterial targets can be developed, any given compound may have toxic targets in the human host. This study nonetheless highlights the utility of combining an *in vivo* MOA assay with medicinal chemistry to study the antibacterial mechanisms of molecules.

MATERIALS AND METHODS

Construction of the *E. coli* JP313 $\Delta toIC$ mutant. The $\Delta toIC$ mutation is derived from strain PB3 and was introduced into strain JP313 by P1 transduction (29, 30). JP313 was transduced to tetracycline resistance with a lysate of strain CAG18475 (*metC162::Tn10*), and the methionine requirement of the transductants was confirmed. This strain was then transduced to prototrophy with a lysate of PB3, and these transductants were screened on MacConkey agar for the presence of the $\Delta toIC$ mutation. Transductants that acquired $\Delta toIC$ were unable to grow on this medium owing to their sensitivity to bile salts such as deoxycholate, and these arose at about 6%, in keeping with previous linkage data (29, 31). PB3 and CAG18475 were obtained from the *Coli* Genetic Stock Center at Yale University.

Synthetic compound library screen. A synthetic small molecule library consisting of ~1,800 compounds was obtained from the ChemBridge EXPRESS-pick library stock collection and screened in 96-well plates at 100 $\mu\text{g}/\text{ml}$ in Luria-Bertani (LB) medium to identify compounds active against the *E. coli* $\Delta toIC$ mutant.

Determining MICs. MICs were determined using the broth microdilution method performed in triplicate. All compounds used in this study were purchased from ChemBridge and solubilized in dimethyl sulfoxide (DMSO). Concentrated stocks of each compound were prepared at 20 mM and stored at -80°C . A 1:100 dilution of an overnight culture of *E. coli* JP313 $\Delta toIC$ mutant was prepared in LB liquid medium and grown at 30°C to an optical density at 600 nm (OD₆₀₀) between 0.2 and 0.4. With the exception of a medium control column, 1 μl of cells diluted to an OD₆₀₀ of 0.05 was added to a 96-well plate containing 2-fold serial dilutions of eight different starting concentrations of each compound in 100 μl of LB medium. An initial cell density count was determined using a plate reader prior to incubation at 30°C for 24 h while shaking. After 24 h, the optical density was determined, and OD₆₀₀ readings were corrected by subtracting the initial reading at T⁰ from the final OD₆₀₀ reading at T²⁴. Readings of 0.5 and below constituted inhibition.

Bacterial cytological profiling. High-resolution fluorescence microscopy and bacterial cytological profiling (BCP) were performed as previously described by Nonejuie et al. (19). Briefly, overnight cultures of the *E. coli* JP313 $\Delta toIC$ mutant were diluted 1:100 in LB medium, followed by incubation with rolling at 30°C until they reached an OD₆₀₀ between 0.15 and 0.17. Next, 300 μl of cells was treated with compounds prepared to the desired test concentration and incubated while rolling at 30°C . Microscopy images were taken after 30 min, 1 h, 2 h, and/or 4 h. Prior to applying the treated culture to an agarose pad for imaging, the cells were stained with FM4-64, DAPI (4',6'-diamidino-2-phenylindole), and SYTOX-green as previously described (19).

Cell viability. Viability assays were performed in triplicate for the *E. coli* JP313 $\Delta toIC$ strain treated with compounds 1 and 2. Cells were plated for colony counting at the same time points used for BCP imaging. The plates were incubated at room temperature overnight, then individual colonies were counted. The number of CFU per milliliter was calculated for each treatment condition. These values were then normalized using the T⁰ measurement of the untreated cells and subsequently log₁₀ transformed. The resulting viability measurements were averaged across three independent trials and plotted with standard errors.

Resistant mutant selection. Mutants resistant to compounds 1 and 2 were obtained via serial passaging. A 1:500 dilution of an overnight culture of the *E. coli* JP313 $\Delta toIC$ strain was prepared in 6 ml of LB medium and incubated at 30°C with rolling until the cells reached an OD₆₀₀ of 0.2 to 0.25. In a small glass culture tube, 1 μl of cells was added to 1 ml of LB medium containing compound at a concentration of $0.5 \times \text{MIC}$. The cultures were incubated at 30°C for 1 day while rolling. If growth occurred at the starting concentration, the culture was diluted 1,000-fold using LB medium containing a slightly higher concentration of compound. Serial passaging was performed until the highest concentration of each compound was reached, at which point colonies were selected and purified from plates containing the compound. Only one mutant colony from each independent culture was selected for sequencing.

Genomic DNA extraction and quantification. Genomic DNA was extracted using a protocol adapted for use with a Qiagen DNeasy blood and tissue kit. The gDNA concentration was quantified using a Thermo Scientific NanoDrop One Microvolume UV-Vis spectrophotometer. gDNA was stored at -20°C .

Genome sequencing, assembly, and variant analyses. The genome sequences of two *E. coli* JP313 ΔtolC mutants were generated using the Illumina MiSeq sequencing platform with a V2 500 paired-end read kit at the La Jolla Institute for Allergy and Immunology Research, San Diego, CA. All sequence processing and analyses were performed in Geneious Prime. Two FastQ files containing forward and reverse sequence read lists were generated for each genome. The files were imported into Geneious and simultaneously paired (input of expected insert size of 500 bp), resulting in a single paired read list. The sequences were trimmed using the BBDuk v38.37 plugin. BBDuk identifies and trims adapters based on presets for Illumina adapters and paired read overhangs, trims the end of sequences based on quality (Q score), and discards short reads and their associated pair mate. Adapter sequences trimmed using presets for Illumina adapters were trimmed from the right end of the sequence with the Kmer length set at 27 with a maximum substitution allotment of 1. A minimum overlap value of 25 was set for adapter trimming based on paired read overhangs. Low-quality sequences were trimmed on both ends with the minimum quality score set at 30, and reads shorter than 30 bp were discarded. After trimming, the paired-end reads were merged into a single read with BBMerge. The resulting merged and unmerged sequences were mapped to the previously sequenced and annotated genome of the *E. coli* JP313 ΔtolC parent strain using the Geneious assembler set to medium sensitivity and to find structural variants, short insertions, and deletions of any size. Further variation analysis was performed with the resulting alignment using the Geneious SNP finder, set to use the bacterial genetic code and the following parameters—a minimum variant frequency of 0.25, a maximum variant *P* value of 6, and a minimum strand-bias *P* value of 5 when exceeding 65% bias—and to calculate an approximate *P* value for identified variants. Visual inspection of these resulting data led to the identification of mutations present in each genome.

Primer design and PCR. Thymidylate kinase DNA templates ($\sim 1,099$ bp) were amplified from *E. coli* JP313 ΔtolC strains using a Q5 high-fidelity DNA PCR (New England Biolabs). The primers used for these reactions were EM029-TMKF1 (5'-ATGGCAAACCTTCTCGTG-3') and EM030-TMKR1 (5'-GGGTAGTAATCGGGATG-3'). Each PCR mixture (50 μl) contained 100 ng of template genomic DNA, 500 pmol of each primer, and 200 μM deoxynucleoside triphosphates. The thermocycling conditions were 30 s of initial denaturation at 98°C , followed by 30 cycles of denaturation (98°C , 10 s), annealing (61°C , 15 s), and extension (72°C , 2 min). A final extension was performed at 72°C for 5 min. PCR products were purified with the oligonucleotide cleanup protocol, as described in the Monarch PCR & DNA cleanup kit (5 μg) user manual (NEB, T1030). Purified PCR products were sequenced using Sanger methods by Eton Biosciences and trimmed for quality prior to analysis.

***E. coli* genome manipulation by P1 virulent transduction.** P1 transductions of the *tmk(A69T)* allele were carried out according to the protocol described by Miller and Miller (32). The *tmk(A69T)* mutation was backcrossed into the *E. coli* JP313 ΔtolC strain by cotransduction with the closely linked *fhuE* gene. A P1vir lysate of strain JW1088-5 ($\Delta\text{fhuE764}::\text{kan}$) was used to transduce the original *tmk(A69T)* mutant to kanamycin resistance, and transductants were screened for retention of resistance to compound 2. A P1vir lysate of one such transductant was then used to transduce the *E. coli* JP313 ΔtolC strain to kanamycin resistance. Colonies that were also resistant to compound 2, having acquired the *tmk(A69T)* mutation by cotransduction, represented the desired backcross. JW1088-5 was obtained from the Coli Genetic Stock Center at Yale University.

TMK expression in the *E. coli* JP313 ΔtolC mutant. Three full-length *E. coli* K-12 MG1655 thymidylate kinase alleles (wild type, Q45P, and A69T) were amplified and cloned into the plasmid expression vector pRSFDuet-1 (GenScript). Expression is under the control of the T7 *lac* promoter. Plasmids were transformed into the *E. coli* JP313 ΔtolC strain to give the following strains: JP313 ΔtolC -pRSFDuet, JP313 ΔtolC -pRSFDuet-*tmk*⁺, JP313 ΔtolC -pRSFDuet-*tmk*-134, and JP313 ΔtolC -pRSFDuet-*tmk*-205.

These strains were grown in LB medium in the presence of kanamycin (30 $\mu\text{g}/\text{ml}$) to an OD_{600} of 0.1 to 0.2 and then treated with the compounds. The assay was performed with eight different concentrations of each compound, serially diluted 2-fold, in 96-well plates in 100 μl of LB medium with kanamycin at 30 $\mu\text{g}/\text{ml}$. Cell densities were determined using a plate reader before and after a 24-h incubation at 30°C with shaking. Final OD_{600} values were determined by subtracting the values from the initial reading at T^0 . MICs were determined as the lowest concentration of compound resulting in an OD_{600} of 0.5 or below, indicating growth inhibition.

Molecular docking. The protein docking was performed using Autodock Vina (v1.1.2). The crystal structure of *E. coli* thymidylate kinase (TMPK) was obtained in complex with P1-(5'-adenosyl)-P5-(5'-thymidyl)pentaphosphate and P1-(5'-adenosyl)P5-[5'-(3'-azido-3'-deoxythymidine)] pentaphosphate from the Protein Data Bank (PDB 4TMK) (26). Water molecules, cofactors, and the originally docked ligand were removed, while polar hydrogens and partial charges were added using Autodock Tools (v1.5.6), which is available as a part of MGLtools v1.5.6 through The Scripps Research Institute (<http://mgltools.scripps.edu/downloads>). Docking was carried out according to the standard procedures for Autodock Vina, and the resulting docking configuration was viewed and illustrated using Chimera X (<https://www.rbvi.ucsf.edu/chimera/x/>) (33).

***E. coli* TMPK IC_{50} determination.** Inhibition of *E. coli* TMPK catalysis was measured in the direction of ATP synthesis using an ATPlite luminescence assay (Perkin-Elmer, catalog no. 6016739) in white 384-well plates (Corning catalog no. 3825). The assay buffer consisted of 50 mM HEPES (pH 8.0), 25 mM sodium acetate, 10 mM MgCl_2 , 5 mM dithiothreitol, 0.01% Triton X-100, and 0.5 mM EDTA. The dTDP and ADP concentrations were 65 and 10 mM, respectively. The TMPK concentration was 400 pM. Test compounds stock

solutions were prepared at 10 μ M in DMSO. Serial 2-fold dilutions were prepared in buffer supplemented with DMSO such that the final DMSO concentration in the assay was constant at 0.33% and the highest compound concentration tested was 33 μ M. A replicate plate was prepared with no TMPK to serve as the 100% inhibition control and to allow correction for signal suppression by the test compounds, according to the method described by Shapiro et al. (34). The assay volume during the 1-h TMPK reaction was 10 μ l. The reactions were quenched by the addition of 5 μ l of ATPlite reagent. Background luminescence was measured in wells containing only buffer and ATPlite reagent. Luminescence was measured, after 5 min of incubation in the dark, using a Pherastar FS plate reader (BMG Labtech), with 1-s integration/well.

The IC₅₀ values were calculated as follows. The average luminescence of the background wells was subtracted from the luminescence of all the other wells. The correction for signal suppression was made using the data from the plate with no TMPK. The average uninhibited control luminescence (MAX) was measured in the wells containing TMPK but no inhibitor. The average fully inhibited control (MIN) was measured in the wells containing no inhibitor or TMPK. The percent inhibition at each inhibitor concentration was calculated for each compound using the following equation: % inhibition = 100[1 - (X - MIN)/(MAX - MIN)], where X is the measurement in the well with TMPK and the specific concentration of inhibitor. The IC₅₀ was calculated by nonlinear regression from the % inhibition data using the Excel add-on XLfit (ID Business Solutions, Ltd., UK), equation 205, in which the minimum and maximum percent inhibitions are fixed at 0 and 100, respectively, as follows: % inhibition = 100[1/(IC₅₀ⁿ + [I]ⁿ)], where [I] is the inhibitor concentration and n is the Hill slope.

SUPPLEMENTAL MATERIAL

Supplemental material is available online only.

SUPPLEMENTAL FILE 1, PDF file, 3.5 MB.

ACKNOWLEDGMENTS

These studies were supported by the National Institutes of Health (RO1AI117712).

K.P. and J.P. have an equity interest in Linnaeus Bioscience, Inc., and receive consulting income from the company. The terms of this arrangement have been reviewed and approved by the University of California—San Diego in accordance with its conflict-of-interest policies.

E.T.M., J.F.N., J.S., E.E., A.B.S., H.T., and A.I.D. conducted experiments and analyzed data. The manuscript was written by E.T.M., J.F.N., A.I.D., K.P., and J.P. All authors have read and approved the manuscript.

REFERENCES

- Wencewicz TA. 2019. Crossroads of antibiotic resistance and biosynthesis. *J Mol Biol* 431:3370–3399. <https://doi.org/10.1016/j.jmb.2019.06.033>.
- Brown ED, Wright GD. 2016. Antibacterial drug discovery in the resistance era. *Nature* 529:336–343. <https://doi.org/10.1038/nature17042>.
- Pogue JM, Kaye KS, Cohen DA, Marchaim D. 2015. Appropriate antimicrobial therapy in the era of multidrug-resistant human pathogens. *Clin Microbiol Infect* 21:302–312. <https://doi.org/10.1016/j.cmi.2014.12.025>.
- Humphries RM, Yang S, Hemarajata P, Ward KW, Hindler JA, Miller SA, Gregson A. 2015. First report of ceftazidime-avibactam resistance in a KPC-3-expressing *Klebsiella pneumoniae* isolate. *Antimicrob Agents Chemother* 59:6605–6607. <https://doi.org/10.1128/AAC.01165-15>.
- Dougherty TJ, Pucci MJ. 2014. Antibiotic discovery and development. Springer, New York, NY. <https://doi.org/10.1007/978-1-4614-1400-1>.
- Ventola CL. 2015. The antibiotic resistance crisis: part 1: causes and threats. *PT* 40:277–283.
- Livermore DM, Blaser M, Carrs O, Cassell G, Fishman N, Guidos R, Levy S, Powers J, Norrby R, Tillotson G, Davies R, Projan S, Dawson M, Monnet D, Keogh-Brown M, Hand K, Garner S, Findlay D, Morel C, Wise R, Bax R, Burke F, Chopra I, Czaplewski L, Finch R, Livermore D, Piddock LJV, White T, on behalf of the British Society for Antimicrobial Chemotherapy Working Party on The Urgent Need: Regenerating Antibacterial Drug Development. 2011. Discovery research: the scientific challenge of finding new antibiotics. *J Antimicrob Chemother* 66:1941–1944. <https://doi.org/10.1093/jac/dkr262>.
- Lewis K. 2013. Platforms for antibiotic discovery. *Nat Rev Drug Discov* 12:371–387. <https://doi.org/10.1038/nrd3975>.
- Hede K. 2014. Antibiotic resistance: an infectious arms race. *Nature* 509: S2–S3. <https://doi.org/10.1038/509S2a>.
- Frieri M, Kumar K, Boutin A. 2017. Antibiotic resistance. *J Infect Public Health* 10:369–378. <https://doi.org/10.1016/j.jiph.2016.08.007>.
- da Cunha R, Fonseca LP, Calado CRC. 2019. Antibiotic discovery: where have we come from, where do we go? *Antibiotics* 8:45. <https://doi.org/10.3390/antibiotics8020045>.
- Newman D. 2017. Screening and identification of novel biologically active natural compounds. *F1000Res* 6:783. <https://doi.org/10.12688/f1000research.11221.1>.
- Hughes JP, Rees S, Kalindjian SB, Philpott KL. 2011. Principles of early drug discovery. *Br J Pharmacol* 162:1239–1249. <https://doi.org/10.1111/j.1476-5381.2010.01127.x>.
- Baell J, Walters MA. 2014. Chemistry: chemical con artists foil drug discovery. *Nature News* 513:481–483. <https://doi.org/10.1038/513481a>.
- Tomasic T, Peterlin Masic L. 2012. Rhodanine as a scaffold in drug discovery: a critical review of its biological activities and mechanisms of target modulation. *Expert Opin Drug Discov* 7:549–560. <https://doi.org/10.1517/17460441.2012.688743>.
- Baell JB, Nissink JWM. 2018. Seven year itch: pan-assay interference compounds (PAINS) in 2017—utility and limitations. *ACS Chem Biol* 13:36–44. <https://doi.org/10.1021/acschembio.7b00903>.
- Baell JB, Holloway GA. 2010. New substructure filters for removal of pan assay interference compounds (PAINS) from screening libraries and for their exclusion in bioassays. *J Med Chem* 53:2719–2740. <https://doi.org/10.1021/jm901137j>.
- Lamsa A, Liu WT, Dorrestein PC, Pogliano K. 2012. The *Bacillus subtilis* cannibalism toxin SDP collapses the proton motive force and induces autolysis. *Mol Microbiol* 84:486–500. <https://doi.org/10.1111/j.1365-2958.2012.08038.x>.
- Nonejuie P, Burkart M, Pogliano K, Pogliano J. 2013. Bacterial cytological profiling rapidly identifies the cellular pathways targeted by antibacterial molecules. *Proc Natl Acad Sci U S A* 110:16169–16174. <https://doi.org/10.1073/pnas.1311066110>.

20. Htoo HH, Brumage L, Chaikeratisak V, Tsunemoto H, Sugie J, Tribuddharat C, Pogliano J, Nonejuie P. 2019. Bacterial cytological profiling as a tool to study mechanisms of action of antibiotics that are active against *Acinetobacter baumannii*. *Antimicrob Agents Chemother* 63:e02310-18. <https://doi.org/10.1128/AAC.02310-18>.
21. Lamsa A, Lopez-Garrido J, Quach D, Riley EP, Pogliano J, Pogliano K. 2016. Rapid inhibition profiling in *Bacillus subtilis* to identify the mechanism of action of new antimicrobials. *ACS Chem Biol* 11:2222-2231. <https://doi.org/10.1021/acscchembio.5b01050>.
22. Nonejuie P, Trial RM, Newton GL, Lamsa A, Ranmali Perera V, Aguilar J, Liu WT, Dorrestein PC, Pogliano J, Pogliano K. 2016. Application of bacterial cytological profiling to crude natural product extracts reveals the antibacterial arsenal of *Bacillus subtilis*. *J Antibiot (Tokyo)* 69:353-361. <https://doi.org/10.1038/ja.2015.116>.
23. Peters CE, Lamsa A, Liu RB, Quach D, Sugie J, Brumage L, Pogliano J, Lopez-Garrido J, Pogliano K. 2018. Rapid inhibition profiling identifies a keystone target in the nucleotide biosynthesis pathway. *ACS Chem Biol* 13:3251-3258. <https://doi.org/10.1021/acscchembio.8b00273>.
24. Martinez-Botella G, Breen JN, Duffy JE, Dumas J, Geng B, Gowers IK, Green OM, Guler S, Hentemann MF, Hernandez-Juan FA, Joseph-McCarthy D, Kawatkar S, Larsen NA, Lazari O, Loch JT, Macritchie JA, McKenzie AR, Newman JV, Olivier NB, Otterson LG, Owens AP, Read J, Sheppard DW, Keating TA. 2012. Discovery of selective and potent inhibitors of gram-positive bacterial thymidylate kinase (TMK). *J Med Chem* 55:10010-10021. <https://doi.org/10.1021/jm3011806>.
25. Keating TA, Newman JV, Olivier NB, Otterson LG, Andrews B, Boriack-Sjodin PA, Breen JN, Doig P, Dumas J, Gangl E, Green OM, Guler SY, Hentemann MF, Joseph-McCarthy D, Kawatkar S, Kutschke A, Loch JT, McKenzie AR, Pradeepan S, Prasad S, Martinez-Botella G. 2012. *In vivo* validation of thymidylate kinase (TMK) with a rationally designed, selective antibacterial compound. *ACS Chem Biol* 7:1866-1872. <https://doi.org/10.1021/cb300316n>.
26. Lavie A, Ostermann N, Brundiens R, Goody RS, Reinstein J, Konrad M, Schlichting I. 1998. Structural basis for efficient phosphorylation of 3'-azidothymidine monophosphate by *Escherichia coli* thymidylate kinase. *Proc Natl Acad Sci U S A* 95:14045-14050. <https://doi.org/10.1073/pnas.95.24.14045>.
27. Haouz A, Vanheusden V, Munier-Lehmann H, Froeyen M, Herdewijn P, Van Calenbergh S, Delarue M. 2003. Enzymatic and structural analysis of inhibitors designed against *Mycobacterium tuberculosis* thymidylate kinase new insights into the phosphoryl transfer mechanism. *J Biol Chem* 278:4963-4971. <https://doi.org/10.1074/jbc.M209630200>.
28. Zgurskaya HI, Lopez CA, Gnanakaran S. 2015. Permeability barrier of gram-negative cell envelopes and approaches to bypass it. *ACS Infect Dis* 1:512-522. <https://doi.org/10.1021/acscinfecdis.5b00097>.
29. Whitney EN. 1971. The *tolC* locus in *Escherichia coli* K-12. *Genetics* 67:39-53. <https://doi.org/10.1093/genetics/67.1.39>.
30. Economou A, Pogliano JA, Beckwith J, Oliver DB, Wickner W. 1995. SecA membrane cycling at SecYEG is driven by distinct ATP binding and hydrolysis events and is regulated by SecD and SecE. *Cell* 83:1171-1181. [https://doi.org/10.1016/0092-8674\(95\)90143-4](https://doi.org/10.1016/0092-8674(95)90143-4).
31. Morona R, Reeves P. 1981. Molecular cloning of the *tolC* locus of *Escherichia coli* K-12 with the use of transposon Tn10. *Mol Gen Genet* 184:430-433. <https://doi.org/10.1007/BF00352517>.
32. Miller JH, Miller JB. 1972. *Experiments in molecular genetics*. Cold Spring Harbor Laboratory, Cold Spring Harbor, NY.
33. Goddard TD, Huang CC, Meng EC, Pettersen EF, Couch GS, Morris JH, Ferrin TE. 2018. UCSF ChimeraX: meeting modern challenges in visualization and analysis. *Protein Sci* 27:14-25. <https://doi.org/10.1002/pro.3235>.
34. Shapiro AB, Walkup GK, Keating TA. 2009. Correction for interference by test samples in high-throughput assays. *J Biomol Screen* 14:1008-1016. <https://doi.org/10.1177/1087057109341768>.